

Comparative Study on the Stability of SBS Modified Asphalt with M Resin Replacing Sulfur

Zhen Lei
School of
Transportation
and
Vehicle
Engineering
Shandong
University of
Technology
Zibo, China

Jinyi Lu
Shandong
Tongzhou
Engineering Con
sulting Co., Ltd.
Zibo Branch,
Zibo, China

Zhirong Jia*
School of Civil
and Architecture
Engineering
Shandong
University of
Technology
Zibo, China

Chaoyu Li
School of
Transportation
and Vehicle
Engineering
Shandong
University of
Technology
Zibo, China

Xuefeng Lin
School of
Transportation
and Vehicle
Engineering
Shandong
University of
Technology
Zibo, China

Abstract: In order to compare the difference between M resin and sulfur modified asphalt stabilizer, two stabilizers were prepared according to the mass ratio of sulfur is 75%, tetramethylthiuram disulfide is 20%, and zinc oxide is 5%. The resin is equivalently incorporated in such a way that the sulfur mass remains unchanged. The softening point, penetration, 5 °C ductility, and 48-hour softening point difference index of the modified asphalt were measured in five cases: 0%, 0.05%, 0.10%, 0.15%, and 0.2%. The change law of each index, and the physical dispersion state of SBS modified asphalt was compared by fluorescence microscope. The test results show that with the increase of the amount of the two stabilizers, the softening point of the modified asphalt increases, the penetration degree decreases, the softening point difference at 48 hours decreases, and the ductility at 5 °C increases first and then decreases; M resin-based stabilizers and The optimal blending amount of sulfur-based stabilizers is 0.15%; under the optimal blending amount, compared with sulfur-based stabilizers, the M resin base has a reduced softening point of modified asphalt of 0.6 °C and an increase in penetration index of 2.2 (0.1 mm), the ductility at 5 °C is reduced by 0.7 cm, and the softening point difference at 48h is increased by 1.4 °C. The sulfur-based stabilizer is slightly better than the M resin-based stabilizer, but the difference is not large. Microscopic analysis also proves the effectiveness of the two stabilizers. It is feasible that M resin replaces sulfur to prepare modified asphalt stabilizer.

Key words: M resin; sulfur; SBS modified asphalt; stabilizer; thermal storage stability

1. INTRODUCTION

M resin is a by-product produced during the preparation of rubber accelerator M by a high-pressure method. M resin is yellow viscous at normal temperature, has no fluidity, and is a hazardous solid waste containing sulfur.

M resin is difficult to handle. Liu Anhua et al. Used M resin, phenol, and formaldehyde as raw materials to copolymerize them into thermoplastic resins^[1]; Yin Zhigang et al. Mixed M resin with sulfur through high temperature and high pressure to generate accelerator M^[2]. Limited by processing cost and technology, M resin is often simply burned, which emits harmful gases such as sulfur dioxide, nitrogen oxides, and hydrogen sulfide, causing air pollution.

n.

Modified asphalt is obtained by adding a certain amount of modifiers such as ethylene-butadiene-styrene block copolymer (SBS) to the matrix asphalt, and its road performance is significantly improved than the matrix asphalt. However, SBS has poor compatibility with matrix asphalt and cannot be stably dispersed. To this end, it is necessary to incorporate sulfur-containing stabilizers to improve thermal storage stability^[3-4]. Due to the high sulfur content of M resin, the total content of elemental sulfur and compound sulfur is about 20% -38%. Therefore, an attempt was made to replace the M resin equivalently with sulfur to prepare a stabilizer. By comparing with the traditional stabilizer.

zer, the stability of the resin Effect, to explore new ways of using M resin waste.

2. MATERIALS

The A-grade 70 # Qilu road petroleum asphalt was selected in this experiment. The basic indicators are shown in Table 1. In the test, SBS with a star and linear ratio of 1: 1 was used as the modifier. The materials used in the test met the requirements of JTGF40-2004 "Technical Specifications for Highway Asphalt Pavements".

Table 1 Asphalt technical index test results

Test items	unit	results	requirements	method
Penetration	0.1mm	69	60~80	T0604-2011
25 °C				
Penetration	---	-1.1	-1.5~+1.0	T0604-2011
Index PI				
Softening	°C	48.6	≥46	T0606-2011
Point				
Ductility	cm	40	≥20	T0605-2011
10 °C, 5cm /				
min				
Ductility	cm	>150	≥100	T0605-2011
5 °C, 5cm /				
min				
density	g/cm ³	1.033	实测值	T0603-2011
60 °C				
dynamic	Pa·S	218	≥180	T0620-2011
viscosity				
Flash point	°C	296	≥260	T0611-2011
Wax content	%	1.6	≤2.2	T0615-2011
Solubility	%	99.94	≥99	T0607-2011
Film oven				
quality	%	-0.07	≠±0.8	T0609-2011
change				

The M resin (A) selected for the test was provided by Shandong Shangshun Chemical Co., Ltd. as a vulcanizing cross-linking agent in the stabilizer; the sulfur used in the test comparison was produced by Tianjin Damao Chemical Reagent Factory with a purity higher than 99.5%; Shanghai Dibo Tetramethylthiuram disulfide (B) produced b

y Chemical Technology Co., Ltd. is used as a vulcanization crosslinking accelerator; zinc oxide (C) produced by Yantai Shuangshuang Chemical Co., Ltd. is used as a vulcanization crosslinking active agent. Among them, Shandong Shangshun Chemical Co., Ltd. commissioned Shanghai Microspectrum Technology Co., Ltd. to perform in-depth micro spectral analysis on the mixture M resin. The microspectra analysis test results are shown in Table 2^[5].

Table 2 M resin microspectrum depth analysis results

Composition	Mass fraction%	Composition	Mass fraction%
water	7.68	Thioisocyanate	0.03
sulfur	18.79	Methylphenyl disulfide	0.89
Thiophenol	0.61	2-acetylbenzothiazole	0.21
Benzothiazole	35.55	2-aminobenzenethiol	0.03
aniline	3.51	4-methyl-5-(5-methyl-1H-pyrazol-3-yl)-1H-1,2,3-triazole	0.07
2-methylbenzothiazole	0.80	Metronidazole	0.05
2-mercaptobenzothiazole	5.08	2,2'-bibenzothiazole	0.83
O-Toluene isothiocyanate	0.05	Triphenylguanidine	0.53
2-methylthiobenzothiazole	1.78	2-[3-(2-thienyl)phenyl] thiophene	1.38
2-hydroxybenzothiazole	0.15	2-(4-aminophenyl)-6-methylbenzothiazole	0.04
Diphenylamine	0.58	Biphenylurea	0.14
3-methyl-2 (3H) -benzothiazolthione	1.27	10-methylphenothiazine	0.09
Phenothiazine	1.04	Quinoline-8-thioamide	0.32
N-phenyl-1,3-benzothiazol-2-amine	17.23	Diphenyl disulfide	0.02
1-methyl-2-phenylbenzimidazole	0.05	Sodium sulfate	1.20

3. EXPERIMENTAL METHOD

3.1 Preparation of SBS modified asphalt

The process is as follows: (1) heating the matrix asphalt to 180 °C and maintaining the temperature constant; (2) weighing 4% of the mass of the matrix asphalt SBS modifier (star type: linear type = 1: 1) and adding to Heat to the flowing matrix

asphalt, and then use a high-speed shearer to shear the SBS modifier into the asphalt at a shear rate of 5000 r / min for 30 minutes; (3) modify the SBS after the shearing is completed. The asphalt was developed in an oven at 180 ° C for 2 hours, during which indirect stirring was performed and two base stabilizers were added.

3.2 Experimental design to determine the effect of stabilizers

According to the previous research, two base stabilizers were prepared according to the mixing ratio of A (M resin (calculated as sulfur) / S): B (TMTD): C (ZnO) = 15: 4: 1, and two base stabilizers were prepared. SBS modified asphalt samples with the amount of 0%, 0.05%, 0.1%, 0.15%, 0.2% (modified asphalt mass fraction), and the softening point, penetration (25 °C), and ductility (5 °C) And 48h softening point index.

4. TEST RESULTS AND ANALYSIS

4.1 Analysis of conventional performance index test results of modified asphalt

In this section, conventional performance indicators such as penetration (25 °C, 100 g, 5 s), softening point, and ductility at 5 °C are tested and analyzed for the prepared M resin-based and sulfur-based stabilizer modified asphalt samples. The effectiveness of the M resin and the effects of the amounts of the two base stabilizers on the softening point, penetration, and ductility at 5 °C were analyzed. The test results are shown in Figures 1-3.

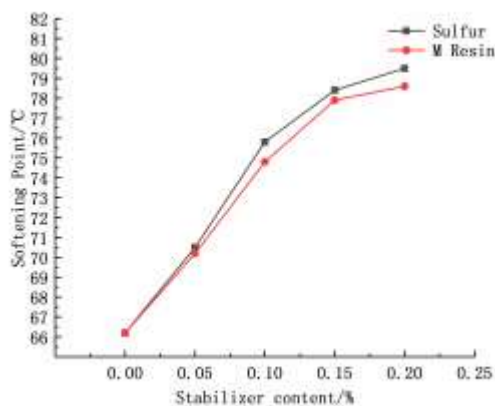


Fig.1 Softening Point Index

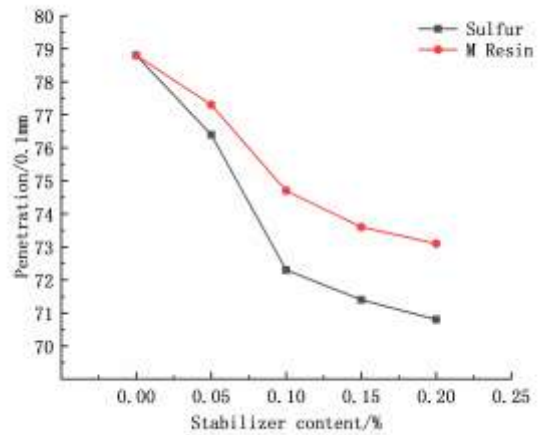


Fig.2 Penetration Index

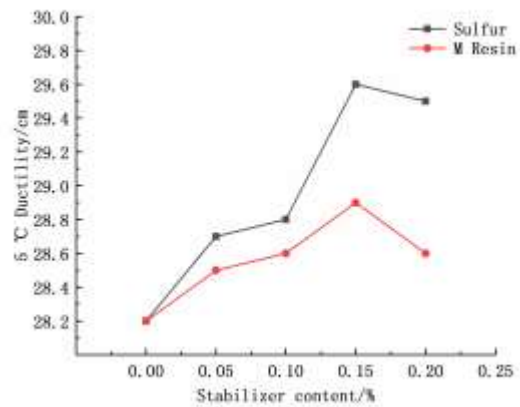


Fig.3 5°Cductility index

As shown in Figure 1, with the increase in the amount of M resin-based stabilizer and sulfur-based stabilizer, the softening point shows an upward trend. Although the increase range is different, it meets the requirements of regularity. After adding M resin-based and sulfur-based stabilizers, the softening point of the modified asphalt can reach above 70 °C.

As shown in Figure 2, the penetration test results of modified asphalt with M resin-based and sulfur-based stabilizers show that the penetration of modified asphalt decreases regularly with the increase in the amount of M resin-based stabilizer. It shows that with the addition of M resin-based and sulfur-based stabilizers and the increase of the amount, the viscosity of the modified asphalt material continues to increase. The penetration test results ranged from 70 to 80 (0.1 mm).

As shown in Figure 3, the ductility index at 5 ° C i ncreases with the increase in the amount of the two base stabilizers from 0% to 0.15%. However, the modified asphalt had slight gelation and the ductility decreased when the content of the two base stabilizers reached 0.2%. The results of the ductility test ranged from 28 to 30 cm.

From the comparative analysis of Figures 1 to 3, it can be seen that when the stabilizer content is increased from 0% to 0.05%, the softening points of sulfur-based and M resin-based stabilizer-modified asphalt are increased by 4.3 °C and 3.9 °C, respectively, and the penetration is reduced. 2.4 and 1.5 (0.1mm), the ductility at 5 °C increased by 0.5 cm and 0.3 cm respectively; when the blending amount was increased from 0.05% to 0.1%, the softening points of sulfur-based and M resin-based stabilizer modified asphalt were increased by 5.3 °C And 4.6 °C, the penetration decreased by 4.1 and 2.6 (0.1mm), and the ductility at 5 °C increased by 0.1 cm and 0.1 cm, respectively; when the blending amount was increased from 0.1% to 0.15%, the sulfur and M resin-based stabilizers The softening point of modified asphalt was increased by 2.6 °C and 3.1 °C, the penetration was decreased by 0.9 and 1.1 (0.1mm), and the ductility at 5 °C was increased by 0.8 cm and 0.3 cm, respectively. The reason for the analysis is that the addition of sulfur-based and M resin-based stabilizers improves the high-temperature performance of modified asphalt, and the softening point and viscosity value are gradually increased, but excessive stabilizers are not conducive to the stable diffusion of stabilizers in the asphalt and asphalt colloids. The structure is transformed into a gel type, which impairs its construction pumping ability. When the stabilizer content is too high, the low temperature crack resistance of asphalt is damaged to a certain extent. On the other hand, the plasticity and strength of the material are two relative indicators. When a higher amount of stabilizer is added to the blending system to increase the strength, the ductility value will decrease to a certain extent. Sulfur-based stabilizers improve the high-temperature performance of modified asphalt better than M resin-based stabilizers. At the same time, the viscosity and low-temperature properties of modified asphalt are stronger than M resin-based stabilizers. M resin is a mixture in which non-sulfur components are mixed between sulfur and polymer to affect the progress of its cross-linking and vulcanization reaction.

4.2 Analysis of test results of thermal storage stability performance index of modified

asphalt

The prepared modified asphalt samples containing M resin-based and sulfur-based stabilizers were tested, and the 48h softening point difference was used as an index to evaluate the thermal storage stability of the modified asphalt. The test data are shown in Tables 3, 4 and Figure 4.

Table 3 Softening point of modified asphalt with different content of M resin-based stabilizer at 48h

M resin-based stabilizer content /%	Separation -48h softening point difference / °C			Note
	1	2	Mean	
	0	35.6	34.0	
0.05	25.8	26.8	26.3	No gelation
0.1	13.8	12.4	13.1	No gelation
0.15	6.7	5.9	6.3	No gelation
0.2	-	-	-	Slight gelation

Table 4 Softening point of modified asphalt with different content of S stabilizer at 48h

M resin-based stabilizer content /%	Separation -48h softening point difference / °C			Note
	1	2	Mean	
	0	35.6	34.0	
0.05	25.2	25.6	25.4	No gelation
0.1	11.6	12.6	12.1	No gelation
0.15	4.2	5.6	4.9	No gelation
0.2	-	-	-	Slight gelation

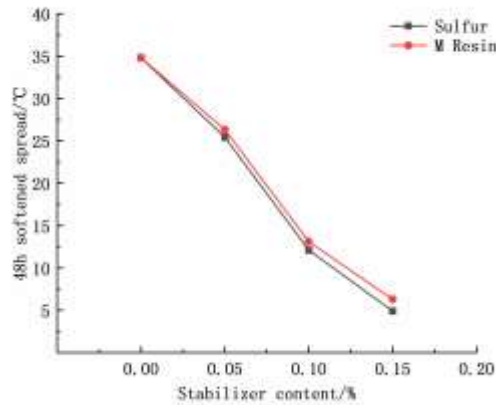


Fig.4 Index of softening spread in 48h

From the data in Tables 3 and 4, and Figure 4, it can be known that with the increase of the amount of M resin-based and sulfur-based stabilizers, the softening point at 48 hours gradually decreases, and its thermal storage stability is improved.

Tables 3 and 4 show that when the blending amount is from 0% to 0.05%, the 48h softening point difference of the M resin-based stabilizer modified asphalt is reduced by 8.5 °C, and the sulfur-based stabilizer modified bitumen is reduced by 9.4 °C. When the blending amount is from 0.05% to 0.1%, the 48h softening point difference with the M resin-based stabilizer is reduced by 13.2 °C, and the 48h softening point difference with the sulfur-based stabilizer is reduced by 13.3 °C; The 48h softening point of M resin-based stabilizer-modified asphalt was reduced by 6.8 °C, and the 48h softening point of sulfur-based stabilizer-modified asphalt was reduced by 7.2 °C. With the addition of the same amount of stabilizer, the M resin-based stabilizer reduced the softening point of modified asphalt at 48h slightly less than the sulfur-based stabilizer, but the gap between the two was small. The reason for this is that the sulfur content of the M resin-based stabilizer and the sulfur-based stabilizer modified asphalt is the same, but because the M resin is a mixture, the addition of non-sulfur components may affect the sulfur modification. The distribution in the asphalt blending system and the progress of the vulcanization reaction, the composition of the M resin substance is more complicated. After researching the various components of the M resin, it was found that the mercaptobenzothiazole and sulfate can be used as vulcanization accelerators. It has a certain effect to promote the vul-

canization cross-linking reaction, which reduces the gap between the M resin-based stabilizer and the sulfur-based stabilizer on the thermal storage stability of the modified asphalt.

4.3 Evaluation of microstructure of modified asphalt

With the help of fluorescence microscopy, the distribution state of the polymer and the matrix asphalt can be observed and recorded, and the homogeneity of the polymer in the asphalt can be analyzed. The prepared modified asphalt samples without stabilizers, M resin-based stabilizers, and sulfur-based stabilizers were photographed at a magnification of 100 times under visible light using a fluorescence microscope, and the microscopic shapes are shown in Figures 5-7.

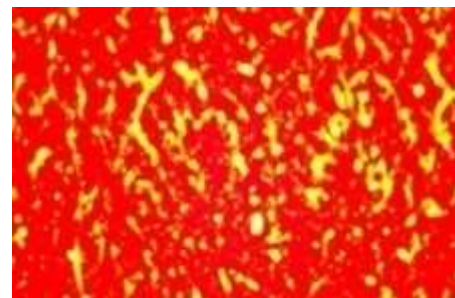


Fig.5 Microstructure of modified asphalt (without stabilizer)

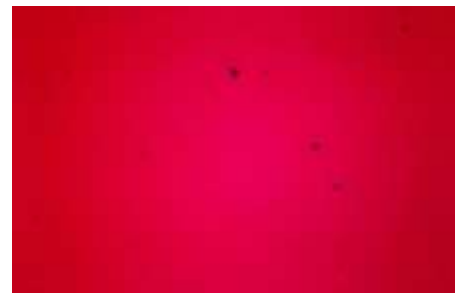


Fig.6 Microstructure of modified asphalt (M resin-based stabilizer)



Fig.7 Microstructure of SBS modified asphalt (with S stabilizer)

From the analysis of the fluorescence photos, it can be known that the SBS modifiers are combined and aggre-

gated with each other in the matrix asphalt by a high-speed shearing machine at a certain temperature. There is no significant difference in the microscope images obtained by adding M resin-based stabilizers and sulfur-based stabilizers under fluorescent irradiation. The polymer distribution is more uniform and better continuity than the microscopic images without stabilizers. The reason is analyzed: the active ingredient in the stabilizer improves the degree of dispersion stability of SBS in asphalt.

5. CONCLUSION

(1) The addition of M resin-based stabilizer improves the softening point and thermal storage stability of the modified asphalt, reduces the penetration, increases the viscosity of the modified asphalt, and the ductility at 5 °C increases from 0% to 0.15%. During the change, it showed an upward trend, and the peak value was 0.15%. When the blending amount is 0.2%, the ductility index at 5 °C decreases, and the modified asphalt slightly gels, which reduces the pumping capacity.

(2) With the addition of the M resin-based stabilizer, SBS is uniformly distributed in the asphalt in the microstructure of the SBS modified asphalt, and the dispersion stability is improved. The SBS performance is effectively transferred to the asphalt, the modification effect is optimized, and the modified asphalt is improved. Performance.

(3) M resin has a higher sulfur content, and non-sulfur components such as mercaptobenzothiazole and sulfates can also promote the crosslinking and vulcanization reaction. According to the comparison of experimental data, M resin can replace the role of sulfur in stabilizers. Participate in the vulcanization cross-linking reaction process in modified asphalt, improve the performance of modified asphalt, and the optimal blending amount of stabilizer for M resin basic formulation is 0.15%.

6. REFERENCES

[1] Liu Anhua, Zhang Lili, Wen Yongxiang. Production of accelerator M and utilization of waste residues[J]. Rubber Industry, 2005, 52(12): 728-730.

[2] Yin Zhigang, Chen Accompanying, Qian Hengyu. Synthesis of Accelerator M and Its Application Progress [J]. Synthetic Rubber Industry, 2007. 30 (5): 398-402.

[3] Yuan Zhongyu, Zhang Wengang, Jia Zhirong, et al. Formulation of direct injection ethylene-butadiene-omitted-ethylene block copolymer modified asphalt stabiliz-

er based on vulcanization mechanism[J]. Science Technology and Engineering, 2018, 18(13): 304-309.

[4] Ouyang Yanqi, Liu Chaohui, Liu Li, et al. Study on thermal storage stability of SBS modified asphalt processed on site[J]. Hunan Transportation Science and Technology, 2019, 45(2): 34-36.

[5] Shandong Shangshun Chemical Co., Ltd. M resin microspectrometry technology report: WP-18052220-FX-01. Shanghai: Shanghai Microspectrometry Technology, 2018.

[6] Giovanni Polacco, Sara Filippi. Vulcanization accelerators as alternative to elemental sulfur to produce storage stable SBS modified asphalts[J]. Construction and Building Materials, 2014, 58: 94-100.

[7] Hu Kui. Quantitative technology and application of microstructure of SBS modified asphalt[D]. Xi'an: Chang'an University, 2013.

[8] Xu Qi. Comparative Study on Performance of SEBS and SBS Modified Asphalt[J]. Aging and Application of Synthetic Materials, 2019, 48(4): 39-44.

[9] Li Jingjing, Shao Leishan, Ni Chunxia, et al. Preparation and thermal storage stability evaluation of coupling functionalized SBS modified asphalt[J]. Petroleum Refining & Chemical Industry, 2019, 50(6): 80-83.

[10] Wang Ming. Microphase analysis of SBS modified asphalt based on fluorescence microscope[J]. Transportation Science and Engineering, 2014, 30(3): 10-14.

[11] Wang Tiebao, Jia Peng, Li Yajuan. Study of the Influence of Stabilizers on the Performance of SBS Modified Asphalt[J]. Petroleum Asphalt, 2008, 22 (5): 6-9.

[12] Zhou Kun, Liu Xizhen, Wang Xinyang, et al. Experimental research on storage stability of SBS modified asphalt [J]. Journal of Shandong Jianzhu University, 2018, 33 (4): 39-44.

Development of a Clothing Sizing System for Benghazi School Girls Students Based on Anthropometric Measurements

Salima A.
Bilhassan
Benghazi
University,
Benghazi,
Libya

Hadeer Berras
Ali
Benghazi
University,
Benghazi,
Libya

Hamida
Boushagour
Benghazi
University,
Benghazi,
Libya

Hend Mohamed
Benghazi
University,
Benghazi,
Libya

Naema
Alobaidy
Benghazi
University,
Benghazi,
Libya

Abstract: Clothing plays an important role in the performance and movement of the human body in different age groups so the development of clothing sizing system is the best way to provide the best suitable size in clothing design. The current project is the fourth step towards the overall objective to develop a clothing sizing system for Libyan children based on anthropometric body measurements of Libyan school children. The aim of the current project is to examine anthropometric measurements for female students in grades seven, eight and nine in the basic education stage, to collect body measurements of school children in Benghazi and analyze those using simple statistical methods to understand the body ranges and variations present for students in the three grades to develop sizing system of these grades. Twenty body dimensions were measured for each student to develop clothing sizing system. The measurements were gathered from a total of 180 students (children of age 12 to 14 years old, females) from four schools in Benghazi. The anthropometric data were analyzed using Minitab program. ANOVA tests were used to identify differences between age groups. The results showed that there are differences between most of the body measurements except the head circumference, shoulder to shoulder length, shoulder to waist length, front body width, back body width, knee height. These differences were taken into account when developing sizing system. Pearson correlation coefficients analysis was carried out to determine the interrelationships between the various body measurements. From these findings it may be concluded that the weight, chest circumference, is very strongly correlated with some other dimensions. The mean values and the standard deviation were used for creating size steps for the size chart. Three kinds of sizes were identified: L (large), M (medium) and S (small).

Keywords: Anthropometric data; sizing system; clothing; schoolchildren; Children anthropometry.

1. INTRODUCTION

Clothing fit is the main objective in the garment development process to ensure user comfort and appearance. It is a complex aspect influenced on one side by the anthropometry and body dimensions of the customer and, in the other, by the appearance and social trends [12].

Anthropometry is the science that measures the range of body size in a population. In order to develop standards and solve variations in body size, many scholars agree on the needs to measure human body dimensions for different reasons such as geographical location, nutrition, ethnic group, etc. Due to this, different countries have their own standard body dimension or size standards. Anthropometric data of country are vital database for clothing design and other design applications. It commonly develops in many other countries of the world [1, 2, 4, 5, 6, 7, 10, 13, 14, 15, 16, 17 and 18].

Based on that, clothing manufacturers produce different garments for intended people from the standard body measurements. This study develops size measurements of

uniform school clothing for Benghazi city girls based on data collected from schools in the city.

This study is motivated by the need to examine anthropometric measurements among school children in Libya; to develop garment sizing systems for Libyan school students. The aim of the current study is to examine anthropometric measurements for female students in grades seven, eight and nine in the basic education stage, to collect body measurements of school children and analyze those using simple statistical methods to understand the body ranges and variations present for students to develop size chart of these grades

2. Methodology

This section explains the material and method used in this research.

2.1 Participants

A sample comprising of 180 female students was identified for participation in this study. The sample was randomly selected from four schools (three public schools and one private school)

in Benghazi during 2017/2018. An equal number of children (60 students) were measured per groups (12 to 14 years). Measurements were taken with the permission of officials and school principals. Table 1 contains a summary of the number of schools and students surveyed.

2.2 The Body Measurements

Based on the objective of this project, only twenty anthropometric dimensions are selected and used to establish the clothing sizing systems for students. These dimensions are selected based on previous studies [1, 5, and 7]. Table 2 and Fig.1 to Fig.3 show the body dimensions. These measurements are used to make different types of clothing such as school uniforms. The measurements were taken from the left or right sides of the body for participants are left-handed or right-handed respectively. However, most of the measurements were taken from the right side of the body. While their anthropometric measurements were taken, respondents wore light cloths to get accurate readings. Respondents were also told not to wear shoes when their height and weight measurements were taken. During anthropometric data measurements, two kinds of equipment were used measuring tape. Readings were also taken two times and the average of the readings was recorded as the actual anthropometric measurements of the respondents.

Table 1. Frequency table of children selected for measuring in the study

School Name	Neighbourhood	Total number measured			Total
		Grade			
		12	13	14	
FTAT ALTHORH	ALSALMANY		45	45	90
ALSHOALH	ARTH ALHIRASA	60	-	-	60
SHBEALIA	ALFOYHAT	-	8	4	12
ALSHRWQ ALAFRIQI	ALSALMANY	-	7	11	18
Total		60	60	60	180

Table 2. The Anthropometric Dimension

No	Body Dimension	No	Body Dimension
1	Weight	11	Shoulder to waist length
2	Height	12	Front body length
3	Head circumference	13	Back body length
4	Neck circumference	14	Waist to hips length
5	Waist circumference	15	Shoulder length
6	Chest circumference	16	Front body width
7	Hip circumference	17	Back body width
8	Arm circumference	18	Calf circumference
9	Shoulder to shoulder length	19	Knee circumference
10	Shoulder to wrist length	20	Outside leg length

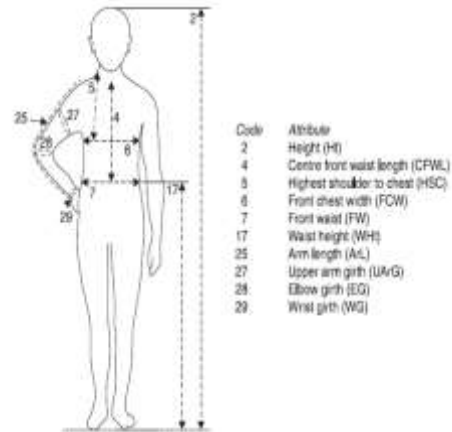


Fig.1 Measures recorded from the front of the body [13]

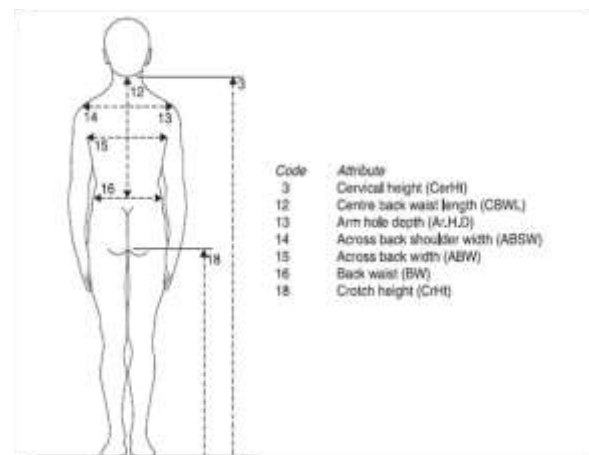


Fig.2 Measures recorded from the back of the body [13]

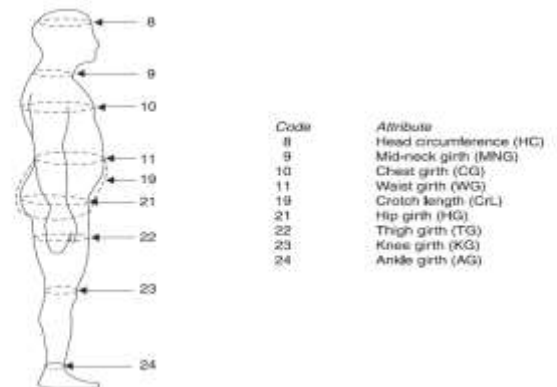


Fig.3 Body girths or circumferences [13]

2.3 Anthropometric Data Analysis

After conducting the anthropometric survey, the data obtained from this study was analyzed using Minitab 17.1 Statistical Package Program for Windows. Descriptive statistics, such as mean, min., max. and standard deviation were used to describe and summarize the data collected. The normality test was used to determine if a data collected is well- modeled by a normal distribution. As expected, data for all measurements followed a normal distribution. Subsequently, ANOVA analysis was carried out to identify differences between age groups. ANOVA was carried out for all dimensions. Moreover, Pearson

correlation coefficients analysis was carried out to determine the interrelationships between the various body measurements. The results from these tests were used to develop the clothing sizing system [1].

3. Results And Discussion

3.1 Descriptive Analysis

As expected that all measurements follow a normal distribution. The mean and standard deviation for all measurements are shown in Table 2. The standard deviation (SD) for almost all dimensions is quite large, showing great variation in the measurements.

Table 2. 2 The mean and standard deviation by age in cm

Body dimensions	Grade		
	7	8	9
1	43.69 (15.63)	53.14 (12.37)	53.77 (4.95)
2	147.27 (8.53)	154.48 (6.28)	157.18 (2.86)
3	54.51 (1.74)	54.88 (1.98)	54.82 (0.11)
4	28.19 (2.53)	31.49 (2.54)	31.7 (4.24)
5	65.74 (13.56)	71.99 (9.98)	70.46 (8.34)
6	70.03 (11.86)	81.58 (9.75)	81.46 (2.16)
7	77.34 (13.06)	88.82 (13.05)	90.31 (2.58)
8	23.19 (4.05)	26.72 (3.57)	26.13 (1.59)
9	37.35 (3.26)	38.63 (3.41)	37.64 (0.81)
10	55.30 (4.87)	54.03 (4.52)	56.62 (0.64)
11	34.84 (3.40)	34.99 (3.60)	35.89 (1.91)
12	32.32 (3.14)	34.46 (3.16)	35.82 (1.66)
13	35.32 (3.02)	37.40 (4.37)	37.89 (2.01)
14	25.84 (3.40)	19.93 (5.12)	24.32 (1.45)
15	11.95 (1.68)	14.13 (1.84)	13.81 (1.45)
16	35.57 (4.82)	36.88 (4.52)	36.29 (4.95)
17	36.98 (22.40)	38.38 (3.62)	36.64 (4.95)
18	30.23 (4.87)	33.67 (3.23)	33.66 (3.57)
19	45.11 (3.58)	45.65 (24.36)	45.05 (1.41)
20	70.55 (6.76)	74.40 (5.84)	75.20 (3.30)

3.2 Differences of Anthropometric Measurements by gender

The results of ANOVA test show that almost all of the anthropometric measurements have significant differences (P-

value < 0.05) between the ages of respondents. These differences would be considered to design clothing sizing systems for different age groups. There are no differences in the Head circumference, Shoulder to shoulder length, Shoulder to waist length, Front body width, Back body width and Knee height between ages groups as shown in Table 3. Therefore, these differences mean that age is one element that influences the development of the human body, and will eventually affect the sizes of clothing [3].

Table 3. Differences of anthropometric measurements by age using ANOVA test

MEASUREMET	F	P-Value	Sig.
Head circumference	0.52	0.593	Not Sig.
Shoulder to shoulder length	2.66	0.073	Not Sig.
Shoulder to waist length	0.89	0.414	Not Sig.
Front body width	1.13	0.325	Not Sig.
Back body width	0.29	0.748	Not Sig.
Knee height	0.03	0.969	Not Sig.

3.3 Correlation Analysis

A key measurement should also be a body measurement with strong relationships with most other body dimensions. Consequently based on this selection, it was possible to develop sizing system. They can be good predictors of the size of other parts of the body. The criteria for key measurements vary and there are various methods to be established in this regard. By using correlation coefficients it could be possible to identify key measurements. Correlation coefficient values indicate the strength of linear relationships between variables and were, as such, implemented in this study.

Pearson correlation coefficients analysis was carried out to determine the interrelationships between the various body measurements. The Pearson correlation coefficient (r) is a measure of the strength of the linear relationship between two random variables. Correlation coefficients range from -1.00 to +1.00. The value of -1.00 represents a perfect negative correlation (indicating a perfect negative linear relationship between variables) and a value of +1.00 represents a perfect positive correlation (indicating a perfect positive linear relationship between variables). A value of 0.00 reflects no correlation (no linear relationship) between the respective variables.

The following arbitrary scale for correlations was implemented to indicate the strength of the relationship between measurements (Gupta and Gangadhar, 2004):

- If correlation coefficient is ,0.5 then no relationship;
- If correlation coefficient is between 0.5 and 0.75 then there is a mild relationship;
- If correlation coefficient is 0.76 it indicates a strong relationship [13].

Table 4 illustrates relationships between measurements and shows the correlation coefficients between each measurement and the other. It is noted that the weight measurement appears to have strong relationships with waist circumference, chest circumference, hip circumference, arm circumference and calf circumference width. Head circumference has strong relationship with waist circumference. Neck circumference has

strong relationship with chest circumference. Waist circumferences have strong relationships with chest circumference and arm circumference. Chest circumference has strong relationships with hip circumference, arm circumference and calf circumference. Arm circumference has strong relationship with calf circumference.

From these findings it may be concluded that weight measurement is the most critical measurement. Weight and chest circumference are key measurements to body garments. In general, it can be inferred that these dimensions are the important landmarks on the body and hence should be related closely to the garment measurements.

Table 4. Correlation coefficients

Measurements	5	6	7	8	18
1	0.836 **	0.899 **	0.798 **	0.845 **	0.833 **
4	0.659 *	0.775 **	0.66* *	0.694 *	0.7* *
5	1	0.842 **	0.737 *	0.788 **	0.755 *
6		1	0.804 **	0.809 **	0.821 **
8				1	0.781 **

3.4 Development of Size Chart

The development of the size chart was carried out using values obtained from the statistical information based on the ANOVA test of body dimensions. The mean values and the standard deviations were used for creating size steps for the size chart. Therefore, different sizes of clothing for girls aged 12, 13 and 14 years must be developed due to the differences in some measurements between age groups. Three sizes were developed: S (small), M (medium) and L (large). These sizes were developed because of there were multiple body shape in each group of 12, 13 and 14 years old.

Three-size steps approach was used to develop the size chart for all body dimensions. To obtain three steps for three categories of body sizes, two standard deviations (2SD) value is added to the mean to obtain one value that is higher than the mean. Two standard deviations (-2SD) values are subtracted from the mean sequentially to obtain one value that is less than the mean for all body dimensions except key body dimensions. There is a difference between ages in height measurement and most of the measurements based on ANOVA analysis. One of the values can be calculated if there is no difference between each parameter. However, three values can be calculated if there is difference between each parameter according to ANOVA.

Table 5 shows the size codes together with the body dimensions. They were calculated into three categories depend on the weight and chest circumference which are very strongly correlated with some of dimensions.

4. Conclusion

The following conclusions were derived

1. As expected that all measurements follow a normal distribution.
2. From the results of ANOVA test, there were differences of anthropometric measurements between age groups except the head circumference, shoulder to shoulder, shoulder to waist length, front body width, back body width and knee height.

3. The key dimensions should be those, which have the strongest correlations with most other body dimensions using Pearson correlation coefficients analysis. From these findings it may be concluded that the weight and chest circumference is very strongly correlated with some of dimensions. In general, it can be inferred that these dimensions are the important landmarks on the body and hence should be related closely to the garment measurements.

The next phase in the ongoing study is to finish gathering anthropometric data and evaluation for the remaining grades in the education stage. After that database for sizing system in the Libya are going to be established.

5. ACKNOWLEDGMENTS

This study is a part of a BSc project of Industrial and manufacturing systems engineering Fall 2017/ 2018, conducted at School of Industrial and Manufacturing Systems Engineering at University of Benghazi. The authors would like to thank all participants for their contributions.

Table 5 Clothing Size Chart of Respondents (CM)

Measurements	S	M	L
1			
12	12.42	43.69	74.96
13	28.40	53.14	77.88
14	43.87	53.77	63.66
2			
12	130.22	147.27	164.32
13	141.92	154.48	167.04
14	151.45	157.18	162.91
3	50.55	54.73	58.91
4			
12	23.13	28.19	33.25
13	26.41	31.49	36.56
14	23.22	31.70	40.19
5			
12	38.61	65.74	92.86
13	52.03	72.00	91.96
14	53.77	70.46	87.15
6			
12	46.30	70.03	93.76
13	62.08	81.58	101.08
14	77.15	81.46	85.78
7			
12	51.22	77.34	103.47
13	62.73	88.82	114.91
14	85.15	90.31	95.47
8			
12	15.08	23.19	31.29
13	19.57	26.72	33.86
14	22.95	26.13	29.32
9	31.43	37.87	44.32
10			
12	45.57	55.30	65.03
13	45.00	54.03	63.07
14	55.35	56.62	57.89
11	25.94	35.24	44.54
12			
12	26.04	32.32	38.61
13	28.14	34.46	40.78
14	32.50	35.82	39.14
13			
12	29.27	35.32	41.36
13	28.66	37.40	46.14
14	33.86	37.89	41.99

Table 5 Cont.

Measurements	S	M	L
14			
12	19.04	25.84	32.64
13	9.69	19.93	30.17
14	21.42	24.32	27.22
15			
12	8.58	11.95	15.32
13	10.45	14.13	17.81
14	10.92	13.81	16.71
16	26.67	36.25	45.82
17	10.84	37.33	63.83
18			
12	20.49	30.23	39.97
13	27.20	33.67	40.14
14	26.52	33.66	40.80
19	16.62	45.27	73.92
20			
12	57.04	70.55	84.06
13	62.72	74.40	86.07
14	68.62	75.20	81.78

6. REFERENCES

- [1] Adu-Boakye, S., Power, J., Wallace, T., Chen, Z. 2012. Development of a Sizing System for Ghanaian Women for the Production of Ready-To-Wear Clothing. In: The 88th Textile Institute World Conference 2012, 15th-17th May 2012, Selangor, Malaysia.
- [2] Alarody, I., Kared, M., Abdelmalek, S. Fall 2015/2016. An anthropometric study to develop clothing charts for Benghazi school-children; BSc Project, Industrial and Manufacturing Systems Engineering Department; University of Benghazi.
- [3] Albarki, F., Bu-Hager, A., Basheer, M., Ali, M., Spring 2017. An anthropometric study to develop clothing charts for seventh, eighth and ninth grades of Benghazi, schoolchildren, BSc Project, Industrial and Manufacturing Systems Engineering Department; University of Benghazi.
- [4] Aminian, O., Negin, R., and Fairuz, I., (2012) Mismatch between anthropometric body dimensions and classroom furniture in Malaysian universities, Canadian engineering education association (CEEA12) Conference.
- [5] Ariadurai, A. S., Nilusha, T. P. G. and Dissanayake, M. R. 2009. An anthropometric study on Sri Lankan school children for developing clothing sizes, Journal of Social Science, 19, 51–56.
- [6] Bari, S., Salleh, N., Sulaiman, N., and Othman, M. 2015. Development of Clothing Size for Pre School Children Based on Anthropometric Measurements, Australian Journal of Sustainable Business and Society, 1(2), 22–32.
- [7] Beazley, A. 1999. Size and fit: The development of size charts for clothing-Part 3, Journal of Fashion Marketing and Management, 3, 66–84.
- [8] Bilhassan, S., ELMABROK, A., ELMHASHHSH, K., Ali, H., Kaddom, A., Elhouni, H. 2018. Development of a Clothing Sizing System for Benghazi Children Based on Anthropometric Measurements, The International Journal of Engineering And Information Technology (IJEIT), 4 (2), 136-140.
- [9] Bilhassan*, S., Albarki, F., Bu-Hager, A., Basheer, M., Ali, M. 2018. An anthropometric study to develop clothing charts for seventh, eighth and ninth grades of Benghazi, schoolchildren, Libyan Journal of Science & Technology, 7(2), 61-64.
- [10] Chung, M.J., Lin, H.F. and Wang, M.J.J. 2007. The development of sizing systems for Taiwanese elementary and high school students, International Journal of Industrial Ergonomics, 37, 707–716.
- [11] Elmabrok, A., Elmehashsh, K., Ali, H., Kaddom, A., Elhouni, H. Fall 2016/2017. Development of a clothing sizing system for Benghazi children based on anthropometric measurements; B.Sc. Project, Industrial and Manufacturing Systems Engineering Department; University of Benghazi.
- [12] Fan, J., Yu, W. and Hunter, L., (2004). Clothing appearance and fit: Science and technology. Woodhead Publishing Limited.
- [13] Gupta, D., Gangadhar, B., R. 2004. A statistical model for developing body size charts for garments', International Journal of Clothing Science and Technology, 16(5), 258–469.
- [14] Gupta, D. and Zakaria, N. 2014. Anthropometry, apparel sizing and design, Woodhead Publishing Limited, UK, 1st Edition.
- [15] Kang, Y., Choi, H., Do, W. H. 2001. A Study of the Apparel Sizing of Children's Wear - An Analysis of the Size Increments Utilized in Children's Wear Based on an Anthropometric Survey', Journal of Korean Home Economics Association English Edition, 2(1), 95–110.
- [16] Lee, Y. 2013. Anthropometric Data Analysis for Body Shape Modeling in Korean, Korean Journal Physics Anthropology, 26(2), 61 – 68.
- [17] Muslim, E., Moch, B., Fileinti, N., Puspasari, M., Siberian, T., Iaksana, D. 2014. The Development of Standard Size for Clothes of Indo-nesian Boys Based on Anthropometric Data as A Reference to Formulate RSNI 055:2013, International Journal of Ergonomics, 4(2), 1–9.
- [18] Zakaria, N. 2011. Sizing System for Functional Clothing-Uniforms for Schoolchildren', Indian Journal of Fiber and Textile Research, 36, 348–357.

Effect of High Level Penetration of Grid Connected Photovoltaic to the Low Voltage Side of the Power System in UK

Safaa Abdulhussein Hasson Al-Abboodi

Ministry of Electricity,

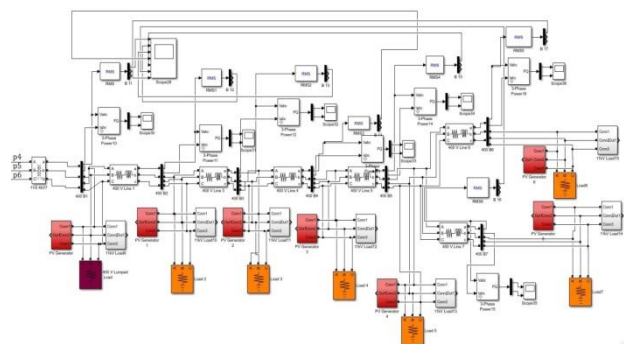
General Company of Electricity for middle

Abstract: This paper analyze the voltage profiles in power distribution networks with different levels of small-scale PV systems. The grid-connected PV system is one of the most promising renewable energy solutions which could offer many benefits to both the end user and the utility network, adistribution network model has been developed in MATLAB/Simulink and implemented to evaluate the voltage profiles and power flow for different levels of PV systems. This will help in evaluating the impact of high penetration levels of small-scale grid connected PV systems on the power quality for a residential distributed network in the UK. Different penetration scenarios and variable load conditions are considered. The result obtained confirmed that maintaining a stable operation and an acceptable power quality in distribution networks are possible with a wide range of PV penetration levels.

Keywords:

1. INTRODUCTION

One of the big challenges are facing the energy sector are increasing energy demands while primary energy sources are limited. Existing power plants are rely mainly on fossil fuels (oil, gas and coal) , which has a negative impact to the environment[1,2]. To overcome these drawbacks, the European commission proposed a new energy policy in 2007 based on distributed generation to reduce the emission of greenhouse gases, improve power quality and increase the contribution of sustainable power sources such as Wind turbine generator and Pv system. However[1,3,4], integration of renewable energy sources to the utility grid introduces a new set of challenges[5,6,7]. As well as, traditional power system is designed as a unidirectional power system, penetration of renewable energy sources at different points of power system require bidirectional power flow and that leading to protection problems[8,6,9,10]. The photovoltaic system and especially (Grid-connected GCPV) are also becoming more prominent during the last few decades[11,12,13]. A typical daily load profile and the output power of 3Kw PV system are considered (summer season). The main issue are expected to be happen is the overvoltage (demand low and generation penetration is high)[3,8,9].



Figure(1): Schematic Diagram of Computer Models (Low voltage side)

2. METHODOLOGY

2.1 Simulation of the UK Distribution Network model

The system modelled by using MATLAB/Simulink simpower system toolbox, the nominal primary voltage is setting to 33kV and supplied to Bus 1. Bus 2 connect to the AC distributed energy sources. Distribution substation in the UK includes two three-phase OLTC regulating transformers rated at 20 MVA, 33 Kv / 11.5 kV type Wye/ Delta. In general, OLTC is located at the primary side of the transformers because of the current will be too less than the current in the secondary side to reduce the spark through transfer between the position of the tap changer. It supplied by medium voltage range 66 or 33kV. The OLTC transformers are used to regulate the system voltage at Bus 2, which is require to change the turn ratio of the transformer. Typical frequency in the UK is setting at 50HZ. The OLTC performed by eight series regulation winding (tapped winding) for each phase. Each phase of the regulating tap windings connected in series with each 11.5/sqrt (3) kV winding. There is inside the OLTC a reversing switch enables reversing connections of the regulation winding. Accordingly, there are Nine OLTC switches works with 17 taps; Zero position, which provides the nominal transformer ratio 33kV/11.5kV, eight negatives (eight subtractive position 1-8) and eight positives (eight additive position 1-8).

The OLTC contained a reverse switching to permit the reverse connection of the regulation winding, which is also connected to ± 8 tap positions.

Each tap in the low voltage side 11.5 kV will maintain a voltage correction of ± 0.0167 pu or $\pm 1.67\%$ of the rated primary voltage 33 kV, as a result, a total of 17 tap positions will permit the variation in voltage by steps of 0.0167 pu (0.55 kV)

The tap changer time response is 5 secs per tap and this is limited by the OLTC controller. As OLTC voltage regulation varied accordingly with a transformer ratio which has a specified dead zone.

The OLTC dead zone ($DZ_{OLTC}=(2)(STEP\ VOLTAGE)$)

Where

Step voltage= Step voltage per tap (per unit)

Therefore, the voltage regulator of the OLTC orders further voltage boosting and stabilises the voltage within a maximum voltage error (which is equal to step voltage), and hence the maximum and minimum permitted of the OLTC is given as:

$$V_{ref} - \left(\frac{DZ_{OLTC}}{2}\right) < V < V_{initial\ tap\ position} + \left(\frac{DZ_{OLTC}}{2}\right)$$

Where

V_{ref} = Reference voltage for the OLTC (per unit)

$V_{initial\ tap\ position}$ = Voltage at initial tap position (per unit)

The maximum and minimum voltage errors per tap changing is set to (0.9875 to 1.0125 per unit) respectively, as the OLTCs value of DZ_{OLTC} has set as 0.025 per unit, and the voltage reference is considered as 1 for each unit.

All distribution transformers had ratio 11/0.433 kV, connected at tap 0%. On a base of 230/400 V. Short circuit level was 500e3 and setting frequency at 50HZ.

Dynamic load emulates as a subsystem block model as shown in Appendix A, Figure 33-A), it includes a lookup table which provide the three phase dynamic load by the required P and Q. Active power P calculated by multiplying the apparent power per 24 hours (Winter and Summer ADMD) by the value of the power factor which supposed (0.95). As well as, reactive power calculated by multiplying the apparent power by the constant which is $(\sin^{-1} \cos 0.95)$.

Domestic PV system output profiles emulates as a subsystem as shown in Appendix A, Figure 33-B), it includes a lookup table which provide the three phase dynamic load by active power only. PV generation values represents inside the lookup table by negative values.

Diesel generator sets emulates as a diesel engine coupled to a synchronous machine as an isolated power source requirements or in scenarios where sudden demand are expected as shown in Appendix B, Figure 34.

3. MODEL SIMULATION WITH DYNAMIC LOAD WITH DIFFERENT PV PENETRATION

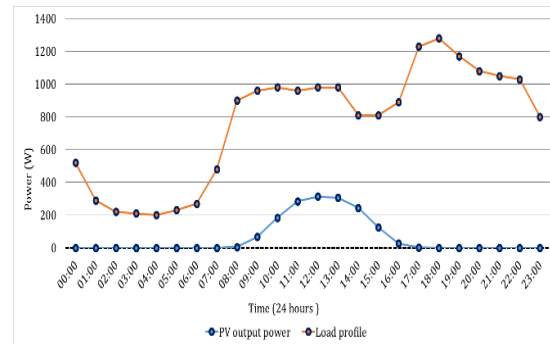
Voltages at different nodes of the distribution network corresponding to the daily load and PV generation profile for a domestic load in the UK adopted.

Domestic PV system output profiles specification for winter and summer was as:

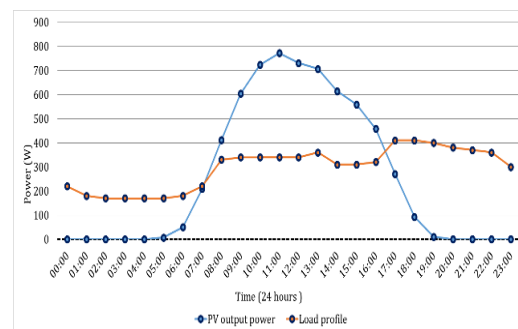
- Winter: generated from the measured output of a domestic PV system in the UK for the months of December, January and February.
- Summer: generated from the measured output of a domestic PV system in the UK for the months of June, July and August.

- System size is 2.03 KW, tilt angle 30 degrees, azimuth angle 0 degrees (south facing), output in Wh (average Wh generated in that hour)-average are calculated for the hour centered on the value, i.e. 10 values are the average output between 9:30 and 10:30.

Many scenarios are achieved by the penetration of the PV on the low voltage side 230/400 V which are 25%, 50% and 100% to each node of the model for a summer and winter profile.



A- Winter season



B- Summer season

Figure 1: Typical daily load profile and PV output power

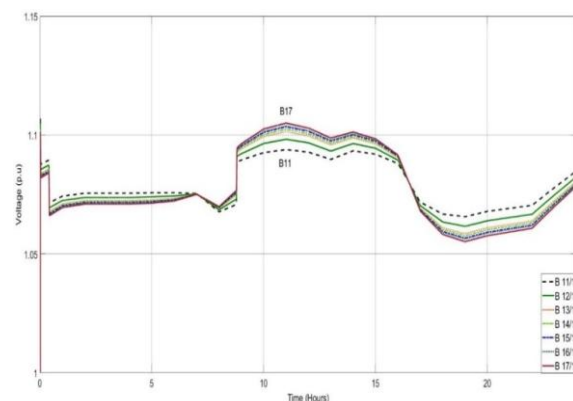


Figure 2: Voltage profile along the 230/400 V feeder with 100% PV penetration level in summer (Off-load tap changer)

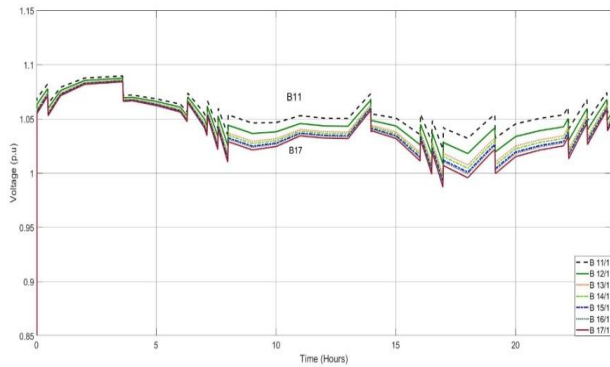


Figure 3: Voltage profile along the 230/400 V feeder with 100 % PV penetration level in winter (On-load tap changer)

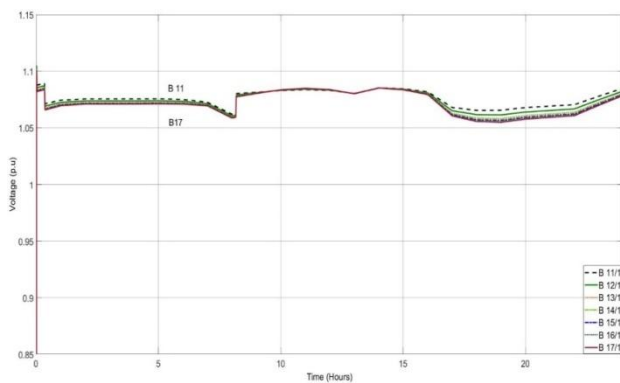


Figure 4: Voltage profile along the 230/400 V feeder with 50 % PV penetration level in summer (On-load tap changer)

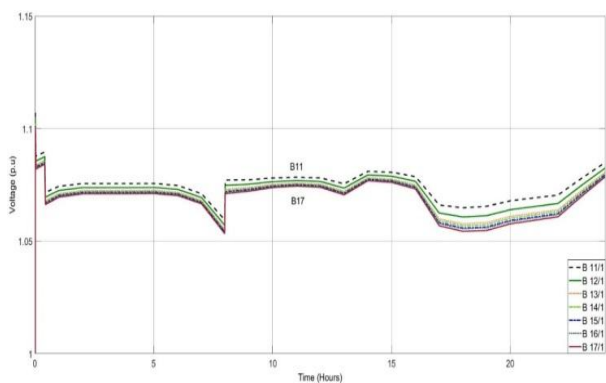


Figure 5: Voltage profile along the 230/400 V feeder with 25 % PV penetration level in summer (On-load tap changer)

4. CONCLUSION

A distribution network model has been implemented and developed in to evaluate the voltage profiles and power flow for different levels of PV systems (25%, 50%, 100%) penetration. It was noticed that even with connecting PV to whole customers (25%, 50%, 100%) penetration in winter, and for (25%, 50%) penetration in summer, the voltage profile sustains on the allowable limits. However, with 100% penetration, the voltage profile exceeds the statutory limit

through the period between (10 AM to 2 PM) in summer where the penetration is 100%, which is considered the best period for PV generation.

The challenge in the renewable distributed generation will be happen when the demand is low, and the penetration level is high, as there might be a bi-directional power flowing according to the location and the capacity of generator, accordingly, these variations can be controlled by utilizing the energy storage systems such as batteries and electric vehicle (EVs) to support the grid by providing the energy when there is a mismatch between the load and the generation. In addition, to save the energy when there is surplus in the generation as compared with demands (particularly in summer season).

5. REFERENCES

- [1] PALZBON, O., KAWHNI, EMI K. & GUERRERO, J. M. 2014. Microgrids in active network management—Part I: Hierarchical control, energy storage, virtual power plants, and market participation. *Renewable and Sustainable Energy Reviews*, 36, 428-439.
- [2] PEI, Y., JIANG, G., YANG, X. & WANG, Z. Auto-master-slave control technique of parallel inverters in distributed AC power systems and UPS. *Power Electronics Specialists Conference, 2004. PESC 04. 2004 IEEE 35th Annual, 2004. IEEE*, 2050-2053.
- [3] PIAGI, P. & LASSETER, R. H. Autonomous control of microgrids. *Power Engineering Society General Meeting, 2006. IEEE, 2006. IEEE*, 8 pp.
- [4] RUA, D., PEREIRA, L. M., GIL, N. & LOPES, J. P. Impact of multi-microgrid communication systems in islanded operation. *Innovative Smart Grid Technologies (ISGT Europe), 2011 2nd IEEE PES International Conference and Exhibition on, 2011. IEEE*, 1-6.
- [5] SALOMONSSON, D., SODER, L. & SANNINO, A. An adaptive control system for a DC microgrid for data centers. *Industry Applications Conference, 2007. 42nd IAS Annual Meeting. Conference Record of the 2007 IEEE, 2007. IEEE*, 2414-2421.
- [6] SIDDIQUI, A. S., MARNAY, C., EDWARDS, J. L., FIRESTONE, R., GHOSH, S. & STADLER, M. 2005. Effects of carbon tax on microgrid combined heat and power adoption. *Journal of Energy Engineering*, 131, 2-25.
- [7] Tushar, M. (2017). Unveiling the Hidden Connections between E-mobility and Smart Microgrid - Optical Zeitgeist Laboratory. [online] Zeitgeistlab.ca. Available at:

- [8]http://www.zeitgeistlab.ca/doc/Unveiling_the_Hidden_Connections_between_E-mobility_and_Smart_Microgrid.html
[Accessed 15 Sep. 2017].
- [9] VASQUEZ, J. C., GUERRERO, J. M., MIRET, J., CASTILLA, M. & DE VICUNA, L. G. 2010. Hierarchical control of intelligent microgrids. *IEEE Industrial Electronics Magazine*, 4, 23-29.
- [10] VISSCHER, K. & DE HAAN, S. W. H. Virtual synchronous machines (VSG's) for frequency stabilisation in future grids with a significant share of decentralized generation. *SmartGrids for Distribution*, 2008. IET-CIRED. CIRED Seminar, 2008. IET, 1-4.
- [11] XINCHUN, L., FENG, F., SHANXU, D., YONG, K. & JIAN, C. The droop characteristic decoupling control of parallel connected UPS with no control interconnection. *Electric Machines and Drives Conference*, 2003. IEMDC'03. IEEE International, 2003. IEEE, 1777-1780.
- [12] YAJUAN, G., WEIYANG, W., XIAOQIANG, G. & HERONG, G. An improved droop controller for grid-connected voltage source inverter in microgrid. *Power Electronics for Distributed Generation Systems (PEDG)*, 2010 2nd IEEE International Symposium on, 2010. IEEE, 823-828.
- [13] ZAMORA, R. & SRIVASTAVA, A. K. 2010. Controls for microgrids with storage: Review, challenges, and research needs. *Renewable and Sustainable Energy Reviews*, 14, 2009-2018.
- [14] ZHANG, Z., HUANG, X., JIANG, J. & WU, B. 2010. A load-sharing control scheme for a microgrid with a fixed frequency inverter. *Electric power systems research*, 80, 311-317.
- [15] ZHONG, Q.-C. & WEISS, G. Static synchronous generators for distributed generation and renewable energy. *Power Systems Conference and Exposition*, 2009. PSCE'09. IEEE/PES, 2009. IEEE, 1-6.